

## Hydrothermal syntheses and structural characterizations of three polyoxomolybdates frameworks linked by M(HL)<sub>2</sub> units (M = Co, Ni, Zn; L = 3-(2-pyridyl)pyrazole)

ZHANG XiuTang<sup>1,4\*</sup>, WU XiaoYuan<sup>3</sup>, SUN DaoFeng<sup>2</sup>, WEI PeiHai<sup>1</sup>, NI ZhongHai<sup>2</sup>,  
DOU JianMin<sup>4</sup>, LI DaCheng<sup>4</sup>, SHI CongWen<sup>1</sup> & HU Bo<sup>1</sup>

<sup>1</sup>Advanced Material Institute of Research, Department of Chemistry and Chemical Engineering,  
Qilu Normal University, Jinan 250013, China

<sup>2</sup>School of Chemistry and Chemical Engineering, Shandong University, Jinan 250100, China

<sup>3</sup>State Key Laboratory of Structural Chemistry; Fujian Institute of Research on the Structure of Matter,  
Chinese Academy of Sciences, Fuzhou 350002, China

<sup>4</sup>College of Chemistry and Chemical Engineering, Liaocheng University, Liaocheng 252059, China

Received January 27, 2010; accepted February 24, 2010; published online June 23, 2010

Three polyoxomolybdate compounds, namely  $\{[M^{II}(HL)_2]_2(Mo_8O_{26})\}_n$  (M = Co (**1**), Ni (**2**), Zn (**3**)) (HL, 3-(2-pyridyl)pyrazole), were designed and synthesized under the hydrothermal conditions and characterized by elemental analysis, IR spectroscopy, and TGA. Single-crystal X-ray diffraction analysis results reveal that compounds **1**–**3** own the isostructural chain structure consisting of the  $\beta\text{-}[Mo_8O_{26}]^{4-}$  anions, which are linked by  $M(HL)_2^{2+}$  units via the terminal oxygen atoms. TGA curves show that the organic ligands separate from the related compounds above ca. 673 K.

**polyoxomolybdate, 3-(2-pyridyl)pyrazole, polyoxomolybdate, cobalt, nickel, zinc**

### 1 Introduction

The design and synthesis of polyoxometalate clusters has attracted continuous research interest not only because of their appealing structural and topological novelty, but also due to their unusual optical, electronic, magnetic, and catalytic properties, as well as their potential medical application [1–16].

The construction of polyoxometalates is usually achieved by the connection of polyoxometalate building subunits either via capping {MO<sub>2</sub>} groups using the two bridging oxygen atoms or by the secondary transition metals, in most cases the transition metal ions exhibiting the M–L (L represents organic ligand) coordination mode [17–20]. The use of

well-defined molecular oxide clusters to construct novel topology with more or less predictable connectivity in the crystal state is attractive, because the secondary metal/ligand bridges should provide sufficiently strong linkages to connect the clusters into stable crystalline architectures. During the past decade, the synthetic methodology of employing organic components to modify the crystallization of metal oxides in a hydrothermal medium has been especially researched [17, 18]. The organic components in these examples usually play the roles of charge-compensating ions and space-filling structural subunits by linking directly to the metal oxide substructure or a secondary metal site as ligands. Based on which, two distinct subgroups of this family have emerged: (i) the molecular structures comprised of polymeric molybdate substructures decorated by the secondary metal-ligand subunit [19, 20]; (ii) the crystal structures are constructed from discrete molybdate clusters

\*Corresponding author (email: xiutangzhang@yahoo.com.cn)

which were bridged by the secondary metal-ligand components, forming chain, network, or framework structures [21, 22]. Consequently, the overall structure reflects both the geometric constraints of the ligand and relative dispositions of the donor groups, as well as the coordination preferences of the secondary metal site. Furthermore, working in the hydrothermal domain allows us to overcome problems associated with the differential solubilities of the reactants. The reduced viscosity of water under these conditions enhances the solvent extraction of solids and the rate of crystallization from solution.

Therefore, the combination modes between polyoxomolybdate subunits and the bridge of M-L or metal oxide framework are worthy of further research because different environments such as temperature and acidity usually lead to interesting structural novelty. As part of our systematic studies of molybdenum/tungsten oxide, we have investigated the hydrothermal chemistry of Tr(II) (transitional metal salts) with molybdate/tungstate salts and nitrogen heterocyclic ligands under a variety of conditions [23–26]. In the present paper, we describe the synthesis and structural characterizations of three polyoxomolybdate chains:  $[M^{II}(HL)_2]_2(Mo_8O_{26})_n$  ( $M = Co$  (**1**),  $Ni$  (**2**),  $Zn$  (**3**)) ( $HL$ , 3-(2-pyridyl)pyrazole).

## 2 Experimental

### 2.1 General experimental

The ligand 3-(2-pyridyl)pyrazole was purchased from Jinan Henghua Sci. & Tec. Co. without further purification. Elemental analysis was conducted on a Perkin-Elmer 240C elemental analyzer; IR spectra were recorded within the 400–4000 cm<sup>-1</sup> region on a Perkin-Elmer 2400LSII spectrometer; Thermogravimetric analysis (TG) was performed on a Perkin-Elmer Diamond TG/DTA instrument.

### 2.2 Synthesis of the 2'-(Se-Me)-adenosine phosphoramidite

#### 2.2.1 Synthesis of compound **1**

The synthesis is performed in 25 mL Teflon-lined stainless steel vessels.  $Na_2MoO_4 \cdot H_2O$  (0.50 mmol, 0.12 g),  $CoCl_2 \cdot 6H_2O$  (0.25 mmol, 0.06 g), 3-(2-pyridyl)pyrazole (0.50 mmol, 0.07 g), and  $H_2O$  (10 mL) were mixed in a molar ratio 2:1:2:550, and the pH value of the mixture was adjusted to ca. 5.0 with 1 M HCl and heated to 150 °C and kept at this temperature for three days. Red block crystals were obtained with the yield of 28%. Anal. Calcd. for  $C_{16}H_{14}CoMo_4N_6O_{13}$ : C, 20.40; H, 1.49; N, 8.93. Found: C, 20.28; H, 1.39; N, 8.79 %. IR (cm<sup>-1</sup>): 3450, 1605, 1429, 1060, 1012, 969, 812, 775, 691, 580, 525.

#### 2.2.2 Synthesis of compound **2**

The synthetic method is similar to that of compound **1** except

that nickel(II) chloride hexahydrate (0.25 mmol, 0.06 g) replaced cobalt(II) chloride hexahydrate. Green block crystals were obtained with the yield of 26%. Anal. Calcd. for  $C_{16}H_{14}Mo_4N_6NiO_{13}$ : C, 20.41; H, 1.49; N, 8.93. Found: C, 20.32; H, 1.41; N, 8.73 %. IR (cm<sup>-1</sup>): 3340, 2925, 1633, 959, 904, 793, 618, 498, 442, 405.

#### 2.2.3 Synthesis of compound **3**

The synthetic method is also similar to that of compound **1** except that zinc(II) acetate dihydrate (0.25 mmol, 0.05 g) replaced cobalt(II) chloride hexahydrate. Colorless block crystals were obtained with the yield of 34%. Anal. Calcd. for  $C_{16}H_{14}Mo_4N_6O_{13}Zn$ : C, 20.26; H, 1.48; N, 8.88. Found: C, 20.18; H, 1.34; N, 8.72 %. IR (cm<sup>-1</sup>): 3450, 2361, 1605, 1577, 1466, 1439, 1374, 1097, 950, 904, 802, 636, 544, 498, 406.

## 2.3 X-ray crystallography

Intensity data collection was carried out on a Siemens SMART diffractometer equipped with a CCD detector using  $MoK\alpha$  monochromatized radiation ( $\lambda = 0.71073 \text{ \AA}$ ) at 293(2) K. The absorption correction was based on multiple and symmetry-equivalent reflections in the data set using the SADABS program based on the method of Blessing. The structures were solved by direct methods and refined by full-matrix least-squares using the SHELLX-TL package [28]. Crystallographic data for compounds **1–3** are given in Table 1. Selected bond lengths and bond angles are listed in Table 3 and Table S1–S2 (supporting Information). For compounds of **1–3**, further details on the crystal structure investigations may be obtained from the Cambridge Crystallographic Data Centre, CCDC, 12 Union Road, CAMBRIDGE CB2 1EZ, UK, [Telephone: +44-(0)1223-762-910, Fax: +44-(0)1223-336-033; Email: deposit@ccdc.cam.ac.uk, http://www.ccdc.cam.ac.uk/deposit], on quoting the depository number CCDC-737019 for **1**, 737020 for **2**, 737021 for **3**.

## 3 Results and discussion

Single crystal X-ray diffraction analyses revealed that these three compounds  $[M^{II}(HL)_2]_2(Mo_8O_{26})_n$  ( $M = Co$  (**1**),  $Ni$  (**2**),  $Zn$  (**3**)) ( $HL$ , 3-(2-pyridyl)pyrazole) crystallize isostructurally, exhibiting the chain structure built up from the  $\beta$ - $Mo_8O_{26}^{4-}$  building blocks joined by two  $M^{2+}$  cations units via terminal oxygen atoms, which are further chelated by two 3-(2-pyridyl) pyrazole ligands via four nitrogen atoms, shown in Figure 1. The octamolybdate polyanion  $Mo_8O_{26}^{4-}$  shows a  $\beta$  configuration with a center of symmetry, which can be bisected into two  $[(\mu_5-O)(Mo_4O_{12})]^{2-}$  planar subunits by Mo-O breaking bonds with the related lengths in the range of 2.26–2.39 Å, similar to previously reported isolated clusters [26]. The  $[(\mu_5-O)(Mo_4O_{12})]^{2-}$  plane could be considered as one Mo atom protrudes outward from the

**Table 1** Crystallographic data and details of diffraction experiments for compounds **1–3**

	<b>1</b>	<b>2</b>	<b>3</b>
Formula	C <sub>16</sub> H <sub>14</sub> CoMo <sub>4</sub> N <sub>6</sub> O <sub>13</sub>	C <sub>16</sub> H <sub>14</sub> Mo <sub>4</sub> N <sub>6</sub> NiO <sub>13</sub>	C <sub>16</sub> H <sub>14</sub> Mo <sub>4</sub> N <sub>6</sub> O <sub>13</sub> Zn
Color	red	green	colorless
Mol. mass (g/mol)	941.02	940.80	947.46
Crystal system	triclinic	triclinic	triclinic
Space group	P-1	P-1	P-1
<i>a</i> (Å)	10.065(3)	10.080(3)	10.0869(7)
<i>b</i> (Å)	11.583(3)	11.589(4)	11.5714(8)
<i>c</i> (Å)	11.583(3)	11.589(4)	11.5714(8)
$\alpha$ (°)	88.79	88.57	89.01
$\beta$ (°)	74.772(2)	74.742(3)	74.677(2)
$\gamma$ (°)	74.772(2)	74.742(3)	74.677(2)
<i>V</i> (Å <sup>3</sup> )	1255.4(6)	1258.7(7)	1254.29(15)
<i>Z</i>	2	2	2
<i>d</i> <sub>calc</sub> (g/cm <sup>3</sup> )	2.489	2.482	2.509
$\mu$ (mm <sup>-1</sup> )	2.667	2.749	2.965
<i>T</i> (K)	298(2)	298(2)	298(2)
Measured refl.	6818	6807	7971
Unique refl.	4593	4593	4355
Refined parameters	361	361	361
2θ range (°)	1.82 to 25.49	1.82 to 25.50	1.83 to 25.00
<i>R</i> [ <i>I</i> >2σ( <i>I</i> )]	<i>R</i> <sub>1</sub> =0.0360 <sup>a)</sup> <i>wR</i> <sub>2</sub> =0.0992 <sup>b)</sup>	<i>R</i> <sub>1</sub> =0.0539 <sup>a)</sup> <i>wR</i> <sub>2</sub> =0.1469 <sup>b)</sup>	<i>R</i> <sub>1</sub> =0.0310 <sup>a)</sup> <i>wR</i> <sub>2</sub> =0.0879 <sup>b)</sup>
<i>R</i> (all data)	<i>R</i> <sub>1</sub> =0.0389 <sup>a)</sup> <i>wR</i> <sub>2</sub> =0.1018 <sup>b)</sup>	<i>R</i> <sub>1</sub> =0.0569 <sup>a)</sup> <i>wR</i> <sub>2</sub> =0.1504 <sup>b)</sup>	<i>R</i> <sub>1</sub> =0.0331 <sup>a)</sup> <i>wR</i> <sub>2</sub> =0.0859 <sup>b)</sup>
Goof <sup>c)</sup>	0.998	1.006	0.997
(Δρ) <sub>max</sub> (e <sup>-</sup> /Å <sup>3</sup> )	0.957	0.983	0.997
(Δρ) <sub>min</sub> (e <sup>-</sup> /Å <sup>3</sup> )	-1.246	-1.090	-0.816

a)  $R_1 = \sum |F_{\text{obsd.}}| - |F_{\text{calcd.}}| / \sum |F_{\text{obsd.}}|$ ; b)  $wR_2 = \{\sum [w(F_{\text{obsd.}}^2 - F_{\text{calcd.}}^2)^2] / \sum [w(F_{\text{obsd.}}^2)^2]\}^{1/2}$ ,  $w = 1 / [\sigma^2(F_o^2) + xP + (yP)^2]$ ; with  $P = (F_o^2 + 2F_c^2)/3$ ; c) goof =  $[\sum w(F_{\text{obsd.}}^2 - F_{\text{calcd.}}^2)^2 / (n-p)]^{1/2}$ , where  $n$ =number of reflections,  $p$ =parameter used.

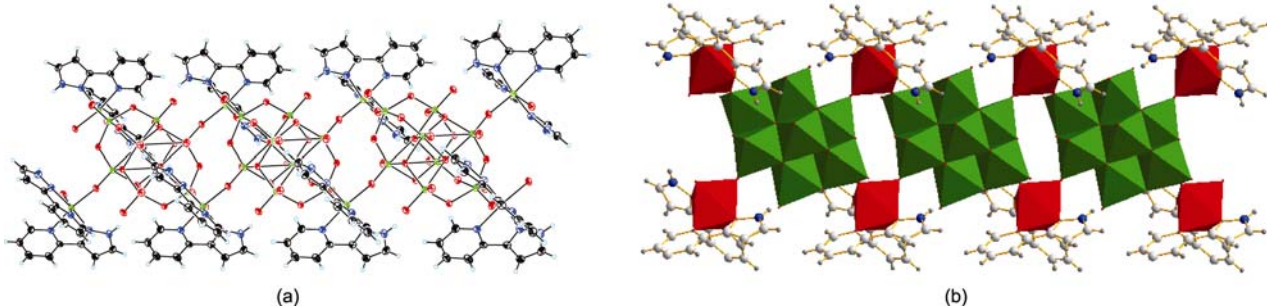


**Figure 1** (a) A view of the chain structure in compounds **1–3**, drawn with 30% probability displacement ellipsoids for the non-hydrogen atoms; (b) a view of the chain structure in compounds **1–3**. The octahedra represent MoO<sub>6</sub> (green) and Mn<sub>4</sub>O<sub>2</sub> (dark red, M=Co, Ni, Zn); the balls are N (blue) and C (gray).

other four Mo constituted planar. There are two types of Mo–O bonds in octamolybdate polyanion: terminal Mo–O, and bridging  $\mu_2$ -O–Mo,  $\mu_3$ -O–Mo, and  $\mu_5$ -O–Mo bonds. The related bond distances vary from the shortest, 1.690 Å for one of the terminal Mo–O bonds, to the longest 2.463 Å for one of the bonds to the unusual  $\mu_5$ -O atom that sits in the

4Mo plane near the center of each Mo–O moiety.

The hexa-coordinated transitional metal cations of Co/Ni/Zn act as a bridge to link two neighboring octamolybdate polyanions, which are further chelated by two 3-(2-pyridyl)pyrazole ligands via four nitrogen atoms. The M–O distances are in the range of 2.076(3)–2.148(3) for Co,

2.067(4)–2.121(4) Å for Ni, 2.105(3)–2.248(3) Å for Zn, respectively. The M–N distances are in the range of 2.073(4)–2.177(3) Å for Co, 2.027(5)–2.134(5) Å for Ni, 2.075(3)–2.248(3) Å for Zn and N(O)–M–N(O) angles 86.48(12)–171.96(14)° for Co, 77.4(2)–173.5(2)° for Ni, 75.26(14)–172.60(14)° for Zn, respectively. The HL group serves as a bidentate ligand to saturate the coordination sites of transitional metal cations Co/Ni/Zn. The nearest Co···Co, and Ni···Ni, Zn···Zn distances along the chain direction are in the range of 7.945–7.982 Å. Thus, the organic subunit of this multi-component system serves to fix a number of coordination sites about the secondary metal ion and to dictate the availability of attachment sites to the oxide clusters. This coordination complex cation not only provides charge

compensation, but also serve space-filling, passivating and structure-directing roles. The coordination preferences of the secondary metal and the geometric and bonding constraints imposed by the ligand may provide structural flexibility, as well as spatial transmission of structural information [19–22].

In addition, it is noteworthy that the multipoint hydrogen-bonding links also exist between the hydrogen atoms from organic amines and the cluster of the surface oxygen atoms from the wave-like chains; this may make a contribution to stabilizing the chain structures of **1–3**, shown in Table 2.

At the final stage of this section, it appears necessary to talk something about the assignment of the oxidation state for the Mo, Co, Ni, and Zn atoms in these compounds, which is

**Table 2** Hydrogen bond lengths (Å) for complexes **1–3**

Compound <b>1</b>		Compound <b>2</b>		Compound <b>3</b>	
bond	dist. (Å)	bond	dist. (Å)	bond	dist. (Å)
N3–H3A···O14	3.069(5)	N1–H1A···O12	3.099(7)	N1–H1A···O1	3.075(5)
N3–H3A···O11	3.047(5)	N1–H1A···O8	3.045(6)	N1–H1A···O3	3.102(4)
N5–H5···O6	2.871(5)	N5–H5A···O5	2.898(7)	N6–H6A···O12	2.842(5)

**Table 3** Selected bond lengths (Å) and angles (°) for complex **1**

Bond	Dist.	Bond	Dist.
Mo(1)-O(11)	1.702(3)	Mo(3)-O(7)	1.893(3)
Mo(1)-O(4)	1.745(3)	Mo(3)-O(2)	1.914(3)
Mo(1)-O(8)	1.946(3)	Mo(4)-O(14)	1.699(3)
Mo(1)-O(3)	1.953(3)	Mo(4)-O(9)	1.721(3)
Mo(1)-O(5)	2.127(3)	Mo(4)-O(2)	1.878(3)
Mo(2)-O(12)	1.701(3)	Mo(4)-O(3)	1.995(3)
Mo(2)-O(6)	1.709(3)	Mo(4)-O(5)	2.275(3)
Mo(2)-O(7)	1.895(3)	Co(1)-N(4)	2.073(4)
Mo(2)-O(8)	2.010(3)	Co(1)-O(9)	2.076(3)
Mo(2)-O(5)	2.310(3)	Co(1)-N(1)	2.081(4)
Mo(3)-O(1)	1.683(3)	Co(1)-N(6)	2.164(4)
Mo(3)-O(10)	1.734(3)	Co(1)-N(2)	2.177(3)
Angle	(°)	Angle	(°)
O(11)-Mo(1)-O(4)	104.84(14)	O(1)-Mo(3)-O(2)	105.22(15)
O(11)-Mo(1)-O(8)	102.45(13)	O(10)-Mo(3)-O(2)	97.31(14)
O(4)-Mo(1)-O(8)	96.95(13)	O(7)-Mo(3)-O(2)	141.03(12)
O(11)-Mo(1)-O(3)	101.00(13)	O(14)-Mo(4)-O(9)	105.89(15)
O(4)-Mo(1)-O(3)	96.25(13)	O(14)-Mo(4)-O(2)	102.26(14)
O(8)-Mo(1)-O(3)	149.05(11)	O(9)-Mo(4)-O(2)	100.15(14)
O(11)-Mo(1)-O(5)	99.34(13)	O(14)-Mo(4)-O(3)	96.30(13)
O(4)-Mo(1)-O(5)	155.80(12)	O(9)-Mo(4)-O(3)	99.89(13)
O(8)-Mo(1)-O(5)	78.49(11)	O(2)-Mo(4)-O(3)	147.68(12)
O(3)-Mo(1)-O(5)	78.02(11)	O(14)-Mo(4)-O(5)	94.26(13)
O(12)-Mo(2)-O(6)	105.09(16)	O(9)-Mo(4)-O(5)	159.52(13)
O(12)-Mo(2)-O(7)	102.35(14)	O(2)-Mo(4)-O(5)	78.66(11)
O(6)-Mo(2)-O(7)	100.49(15)	O(3)-Mo(4)-O(5)	73.73(11)
O(12)-Mo(2)-O(8)	95.00(13)	N(4)-Co(1)-O(9)	90.09(14)
O(6)-Mo(2)-O(8)	100.93(14)	N(4)-Co(1)-N(1)	171.96(14)
O(7)-Mo(2)-O(8)	147.74(11)	O(9)-Co(1)-N(1)	96.30(14)
O(12)-Mo(2)-O(5)	94.65(13)	N(4)-Co(1)-N(6)	75.42(14)
O(6)-Mo(2)-O(5)	159.86(13)	O(9)-Co(1)-N(6)	160.00(13)
O(7)-Mo(2)-O(5)	78.64(11)	N(1)-Co(1)-N(6)	99.47(14)
O(8)-Mo(2)-O(5)	72.97(10)	N(4)-Co(1)-N(2)	97.47(14)
O(1)-Mo(3)-O(10)	104.61(16)	O(9)-Co(1)-N(2)	100.67(13)
O(1)-Mo(3)-O(7)	104.96(15)	N(1)-Co(1)-N(2)	76.59(13)
O(10)-Mo(3)-O(7)	98.35(14)	N(6)-Co(1)-N(2)	94.92(13)

Symmetry transformations used to generate equivalent atoms: #1, -x-1, -y+1, -z+1; #2, -x, -y+1, -z+1.

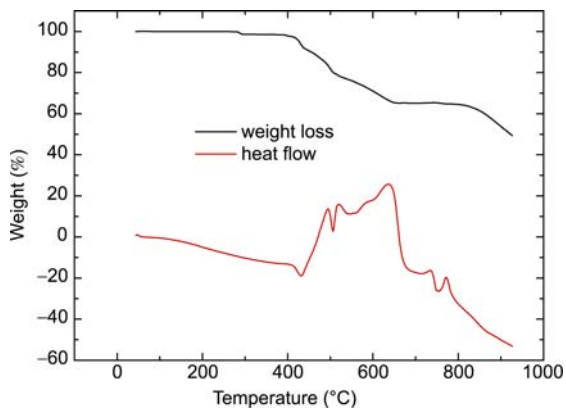


**Figure 2** TG curve for compound 1.

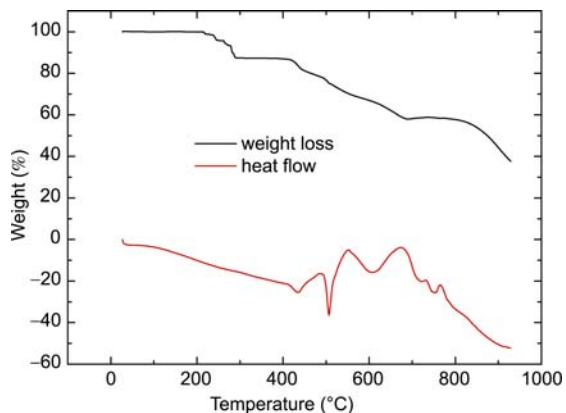


**Figure 3** TG curve for compound 2.

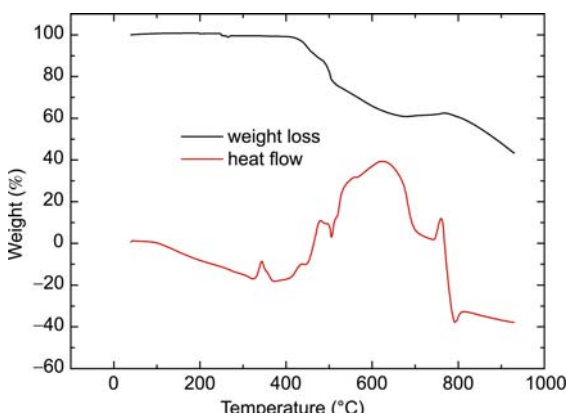


**Figure 4** TG curve for compound 3.

actually consistent with the electric charge confirmed by bond valence sum calculations [27]. By which the valence for the molybdenum atoms is 5.97, 5.91, 5.84, 5.98 for compound **1**; 5.94, 5.82, 5.90, 5.77 for **2**; 5.84, 5.91, 5.96, 5.81 for **3**. The valence for Co, Ni, and Zn atoms is 1.98, 2.01, and 2.10, respectively.

To reveal the thermal stability of compounds **1–3**, TGA measurements have been carried out on a Perkin-Elmer Diamond TG/DTA instrument with a flow of dry air and a

heating rate of 5 °C/min from room temperature to 1000 °C. The TG curves for compounds **1–3** are shown in Figures 2–4. For compounds **1–3**, the TGA curves indicate that the sharp weight loss (32.83%–34.79%) was observed from ca. 673 to 873 K with an obvious endothermal peak, which is attributed to the release of 3-(2-pyridyl)pyrazole ligands coordinated to the first transitional metal cations of cobalt, nickel, and zinc (calcd. 30.61%–30.82%).

#### 4 Conclusions

The successful preparation of three chains represents a confluence of the themes of hydrothermal reaction conditions, organic-inorganic hybrid materials, structural modification by secondary metal/ligand subunits. Further investigations of the optical, electronic, magnetic, and catalytic properties of these newly synthesized compounds are our future research target.

*This work was supported by the Chinese Academy of Sciences ("Hundred Talents Program") and Ministry of Science and Technology of China (2007CB607606), Shandong Provincial Education Department and Qilu Normal University.*

- 1 Pope MT, Müller A. Polyoxometalate chemistry: An old field with new dimensions in several disciplines. *Angew Chem Int Ed Engl*, 1991, 30(1): 34–38
- 2 Ettedgui J, Neumann R. Phenanthroline decorated by a crown ether as a module for metallorganic–polyoxometalate hybrid catalysts: the wacker type oxidation of alkenes with nitrous oxide as terminal oxidant. *J Am Chem Soc*, 2009, 131(1): 4–5
- 3 Pope MT, Müller A. *Polyoxometalates: From Platonic Solids to Ant-Retroviral Activity*. Dordrecht: Kluwer Academic Publishers, 1994
- 4 Wu CD, Lu CZ, Zhuang HH, Huang JS. Hydrothermal assembly of a novel three-dimensional framework formed by  $[GdMo_{12}O_{42}]^{9-}$  anions and nine coordinated  $Gd^{III}$  cations. *J Am Chem Soc*, 2002, 124(15): 3836–3837
- 5 Gaunt AJ, May I, Helliwell M, Richardson S. The first structural and spectroscopic characterization of a neptunyl Polyoxometalate complex. *J Am Chem Soc*, 2002, 124(45): 13350–13351
- 6 Li JY, Liang J, Chen P, Yu JH, Xu Y, Xu RR. Template-designed syntheses of open-framework zinc phosphites with extra-large 24-ring channels. *Cryst Growth Des*, 2008, 8(7): 2318–2323
- 7 Xing HZ, Li JY, Yan WF, Chen P, Jin Z, Yu JH, Dai S, Xu RR. Cogitating ionothermal synthesis of a new open-framework aluminophosphate with unique Al/P ratio of 6/7. *Chem Mater*, 2008, 20(13): 4179–4181
- 8 Sartorel A, Carraro M, Scorrano G, Zorzi RD, Geremia S, Maniel N, Bernhard S, Bonchio M. The first structural and spectroscopic characterization of a neptunyl Polyoxometalate complex. *J Am Chem Soc*, 2008, 130(15): 5006–5007
- 9 Yang WB, Lu CZ, Zhan XP, Zhuang HH. Hydrothermal synthesis of the first vanadomolybdenum polyoxocation with a "Metal-Bonded" spherical framework. *Inorg Chem*, 2002, 41(18): 4621–4623
- 10 Zhai QG, Lu CZ, Wu XJ, Batten SR. Coligand modulated six-, eight-, and ten-connected  $Zn/Cd$ -1,2,4-triazolate frameworks based on mono-, bi-, tri-, penta-, and heptanuclear cluster units. *Crystal Growth & Design*, 2007, 7(11): 2332–2342
- 11 Ettedgui J, Neumann R. Phenanthroline decorated by a crown ether as a module for metallorganic–polyoxometalate hybrid catalysts: The wacker type oxidation of alkenes with nitrous oxide as terminal oxi-

- dant. *J Am Chem Soc*, 2009, 131(1): 4–5
- 12 Han ZG, Zhao YL, Peng J, Gómez-García CJ. Unusual oxidation of an N-Heterocycle ligand in a Metal-Organic framework. *Inorg Chem*, 2007, 46(14): 5453–5455
- 13 Lu CZ, Wu CD, Zhuang HH, Huang JS. Three polymeric frameworks constructed from discrete molybdenum oxide anions and 4,4'-bpy-Bridged linear polymeric copper cations. *Chem Mater*, 2002, 14(6): 2649–2655
- 14 Yin SY, Li W, Wang JF, Wu LX. Mesomorphic structures of protonated surfactant-encapsulated polyoxometalate complexes. *J Phys Chem B*, 2008, 112(13): 3983–3988
- 15 Lee IS, Long JR, Prusiner SB, Safar JG. Selective precipitation of prions by polyoxometalate complexes. *J Am Chem Soc*, 2005, 127(40): 13802–13803
- 16 Jiang K, Zhang HX, Shannon C, Zhan W. Preparation and characterization of polyoxometalate/protein ultrathin films grown on electrode surfaces using layer-by-layer assembly. *Langmuir*, 2008, 24(7): 3584–3589
- 17 Toshihiro Y, Petra VP. Photochemical formation of Tire-Shaped molybdenum blues: topology of a defect anion,  $[Mo_{142}O_{432}H_{28}(H_2O)_{58}]^{12-}$ . *Angew Chem Int Ed*, 2002, 41(3): 466–469
- 18 Mialane P, Duboc C, Marrot J, Rivière E, Dolbecq A, Sécheresse F. Structural and magnetic properties of MnIII and CuII tetrานuclear azido polyoxometalate complexes: Multifrequency high-field EPR spectroscopy of Cu<sub>4</sub> clusters with S=1 and S=2 ground states. *Chem Eur J*, 2006, 12(7): 1950–1959
- 19 Zapf PJ, Hammond RP, Haushalter RC, Zubietta J. Three-dimensional organic/inorganic hybrid materials constructed from one-dimensional copper diamine coordination polymers linked by bridging oxoanion tetrahedra:  $[Cu(dpe)(MoO_4)]$  and  $[Cu(dpe)(SO_4)(H_2O)]$  (dpe = 1,2-*trans*-4-pyridyl)ethene). *Chem Mater*, 1998, 10(5): 1366–1389
- 20 Hagrman D, Haushalter RC, Zubietta J. Three-dimensional organic/inorganic hybrid materials constructed from one-dimensional copper diamine coordination polymers linked by bridging oxoanion tetrahedra:  $[Cu(dpe)(MoO_4)]$  and  $[Cu(dpe)(SO_4)(H_2O)]$  (dpe = 1,2-*trans*-4-pyridyl)ethene). *Chem Mater*, 1998, 10(1): 361–367
- 21 Hagrman PJ, Hagrman D, Zubietta J. Organic-inorganic hybrid materials: From “simple” coordination polymers to organodiamine-templated molybdenum oxides. *Angew Chem Int Ed Engl*, 1999, 38(18): 2638–2803
- 22 Hagrman D, Hagrman PJ, Zubietta J. Solid-State coordination chemistry: The self-assembly of microporous organic-inorganic hybrid frameworks constructed from tetrapyridylporphyrin and bimetallic oxide chains or oxide clusters. *Angew Chem Int Ed Engl*, 1999, 38(21): 3165–3168
- 23 Zhang XT, Dou JM, Wang DQ, Zhou Y, Zhang YX, Li RJ, Yan SS, Ni ZH, Jiang JZ. Divalent manganese linked tungsten–molybdenum polyoxometalates: Synthesis, structure, and magnetic characteristics. *Crystal Growth & Design*, 2007, 7(9): 1699–1705
- 24 Zhang XT, Wang DQ, Dou JM, Yan SS, Yao XX, Jang JZ. Polyoxometalate (W/Mo) compounds connected via lanthanide cations with a three-dimensional framework,  $H_2\{[K(H_2O)_2]_2[Ln(H_2O)_5]_2(H_2M_{12}O_{42})\}_nH_2O$ : Synthesis, structures, and magnetic properties. *Inorg Chem*, 2006, 45(26): 10629–10635
- 25 Zhang XT, Dou JM, Wei PH, Li DC, Li B, Shi CW, Hu B. Synthesis and structural characterizations of four polyoxometalate compounds consisting of transition metals or alkaline cations as the bridging units. *Inorg Chim Acta*, 2009, 362: 3325–3332
- 26 Zhang XT, Wei PH, Sun DF, Ni ZH, Dou JM, Li B, Shi C W, Hu B. Hydrothermal syntheses and structural characterizations of polyoxometalate (Mo/W) compounds consisting of M-L cations, (M=Mn, Co, Ni, Cu, Zn; L=3-(2-pyridyl)pyrazole). *Crystal Growth & Design*, 2009, 9(10): 4424–4428
- 27 Brese NE, O’Keeffe M. Bond-valence parameters for solids. *Acta Crystallogr Sect B*, 1991, 47(2): 192–197
- 28 Sheldrick GM. SHELXTL-97: Program for Refinement of Crystal Structures; University of Göttingen: Göttingen, 1997